Title
Lattice strain accompanying the colossal magnetoresistance effect in EuB6

Journal
Physical Review Letters, 113(6)

ISSN
0031-9007

Authors
Manna, RS
Das, P
De Souza, M
et al.

Publication Date
2014-08-05

DOI
10.1103/PhysRevLett.113.067202

Lattice Strain Accompanying the Colossal Magnetoresistance Effect in EuB_6

Rudra Sekhar Manna,* Pintu Das,† Mariano de Souza,‡ Frank Schnelle, Michael Lang, and Jens Müller§
Institute of Physics, Goethe-University Frankfurt, 60438 Frankfurt (Main), SFB/TR49, Germany

Stephan von Molnár
Department of Physics, Florida State University, Tallahassee, Florida 32306, USA

Zachary Fisk
Department of Physics, University of California, Irvine, California 92697, USA
(Received 4 April 2014; published 5 August 2014)

The coupling of magnetic and electronic degrees of freedom to the crystal lattice in the ferromagnetic semimetal EuB_6, which exhibits a complex ferromagnetic order and a colossal magnetoresistance effect, is studied by high-resolution thermal expansion and magnetostriction experiments. EuB_6 may be viewed as a model system, where pure magnetism-tuned transport and the response of the crystal lattice can be studied in a comparatively simple environment, i.e., not influenced by strong crystal-electric field effects and Jahn-Teller distortions. We find a very large lattice response, quantified by (i) the magnetic Grüneisen parameter, (ii) the spontaneous strain when entering the ferromagnetic region, and (iii) the magnetostriction in the paramagnetic temperature regime. Our analysis reveals that a significant part of the lattice effects originates in the magnetically driven delocalization of charge carriers, consistent with the scenario of percolating magnetic polarons. A strong effect of the formation and dynamics of local magnetic clusters on the lattice parameters is suggested to be a general feature of colossal magnetoresistance materials.

DOI: 10.1103/PhysRevLett.113.067202 PACS numbers: 75.47.Gk, 65.40.De, 74.25.Bt

Materials in which the resistivity exhibits drastic changes in response to an external magnetic field are of great interest both from a fundamental as well as a technological point of view. Those anomalous magnetotransport effects are particularly strongly pronounced close to a combined magnetic and insulator-metal transition, where a large or even a colossal magnetoresistance (CMR) can be observed. Prominent examples include magnetic semiconductors, rare-earth chalcogenides, silicides and hexaborides, Mn-based pyrochlors, as well as the mixed-valent rare-earth manganites [1–6]. One route for describing the CMR effect involves the formation of magnetic polarons (MPs), which are formed when it is energetically favorable for the charge carriers to localize and spin polarize the surrounding local moments over a finite distance. With increasing magnetic field, these ordered clusters may grow in size, accompanied by a progressive alignment of the spins outside the ordered clusters, thereby facilitating the charge transport. The existence of magnetic clusters (tantamount to MPs) in some manganites has been demonstrated by a concomitant lattice distortion, the field dependence of which closely follows the magnetoresistivity [7]. Despite considerable efforts to understand the interplay between spin, charge, and lattice degrees of freedom in the CMR effect for the various materials, see, e.g., Refs. [7–12], no general picture has evolved yet. For the manganites, in particular, the reason for that may be related to their complexity due to the simultaneous action of strong crystal-electric field (CEF) and Jahn-Teller (JT) effects.

Here, we present a detailed study of lattice effects accompanying the CMR effect in the comparatively simple system EuB_6, which—in first order—is devoid of CEF and JT effects. This material has a body-centered cubic structure where B_6 octahedra are surrounded by eight Eu metal atoms residing at the corners of a cube. Because of the Eu^{2+} Hund's rule ground state configuration of $^8S_{7/2}$, which is magnetically isotropic, EuB_6 may be viewed as a model system for studying purely spin-tuned transport phenomena. Despite its simplicity, the system shows a rich phenomenology. The inverse magnetic susceptibility χ^{-1} of the Eu moments shows a linear temperature dependence for $T \gtrsim 20$ K with a paramagnetic (PM) Curie temperature of $\Theta_p \approx 15.6$ K [13,14] and the ferromagnetic (FM) state is reached via two consecutive transitions at $T_{c_1} = 15.3$ K and $T_{c_2} = 12.6$ K [15–18]. Moreover, the PM-FM transition is accompanied by a drastic reduction of the resistance at zero applied field as well as a CMR effect. It has been proposed that the large negative magnetoresistance in EuB_6 at T_{c_1} is a percolation-type transition resulting from the overlap of MPs, which causes a delocalization of the hole carriers [14,16,19]. Upon cooling, the polaronic clusters percolate at $T \leq T_{c_1}$, and finally merge at $T \leq T_{c_2}$, where bulk FM order sets in—a scenario in accordance with recent magnetic [20] and transport data [14,18].

Given the pronounced lattice distortions accompanying the formation of MPs in the manganites, it is natural to look for similar effects also in EuB_6. Surprisingly, only limited information has been available so far on the lattice effects in

EuB_6 [15,21–24]: in T-dependent x-ray diffraction measurements, no significant anomaly at the onset of ferromagnetic order was found [15]. Likewise, a study of x-ray absorption fine structure reported a lack of lattice involvement in the CMR effect [24]. In this Letter, we report on thermal expansion and magnetostriction measurements of EuB_6. Thanks to the significantly higher resolution of these experiments, as compared to the above x-ray studies, we were able to observe a considerable lattice strain disclosing a clear correspondence with the material's CMR effect.

Single crystals of EuB_6 were grown from Al flux as described in Ref. [13]. For the thermal expansion and magnetostriction measurements, a high-resolution capacitive dilatometer (built after Ref. [25]) was used, enabling the detection of length changes $\Delta l \geq 10^{-2}$ Å. This corresponds to a resolution of $\Delta l/l \geq 10^{-10}$, which considerably exceeds the sensitivity of the above-mentioned x-ray experiments of order 10^{-4} [15,24]. The coefficient of thermal expansion $\alpha(T) = d\ln l/dT$ and the magnetostriction coefficient $\lambda = d\ln l/dB$ were obtained along a principal direction of the cubic structure and parallel to the applied magnetic field. The experiments were carried out on two single crystals from different batches yielding similar results. Samples No. 1 and No. 2 have dimensions $5 \times 1 \times 0.75$ mm^3 and $1 \times 0.5 \times 0.2$ mm^3, respectively.

Figure 1(a) shows the thermal expansion coefficient $\alpha(T)$ of EuB_6 and the isostructural LaB_6 [26]. Since the $4f$ shell of La^{3+} is empty, LaB_6 may serve as a nonmagnetic reference system to EuB_6. Consequently, the very large positive contribution to the expansivity for $T \lesssim 15$ K ($\backsimeq T_{c_1}$), corresponding to a strong contraction of the lattice upon cooling through the FM transition, see Fig. 1(b), is of magnetic origin. As observed also for the electrical resistivity, we find two subsequent anomalies in the lattice expansivity. In $\alpha(T)/T$ vs T, shown in the inset of Fig. 1(a), which can be directly compared to literature data of the specific heat C_p/T vs T [15,17], there is a sharp transition at $T_{c_1} = 15.4$ K, corresponding to the λ-shaped anomaly found in the heat capacity and a large maximum below 12 K. From the derivative of the resistivity $d\rho/dT$ [18] and an equal-areas construction in C_p/T vs T (not shown) measured on samples of the same batch, we find $T_{c_2} = 12.6$ K, see arrow in the inset of Fig. 1(a). In order to determine the magnetic contribution α_{mag} to the expansivity of EuB_6, α_{EuB_6}, the phonon contribution α_{ph} has to be subtracted [27]. To this end, we fit the thermal expansion of LaB_6 by a Debye and an Einstein contribution [green curve in Fig. 1(a)], in analogy to the specific heat [28]. We fit the thermal expansion of EuB_6 at $T > 40$ K, where nonphononic contributions can be neglected, by allowing for small changes of the Debye and Einstein temperatures, see the Supplemental Material for details [29].

In Fig. 1(b) we show the relative length change $\Delta l/l$ of EuB_6 as the difference $\epsilon(T) = (\Delta l/l)_{EuB_6} - (\Delta l/l)_{\mathrm{ph}}$,

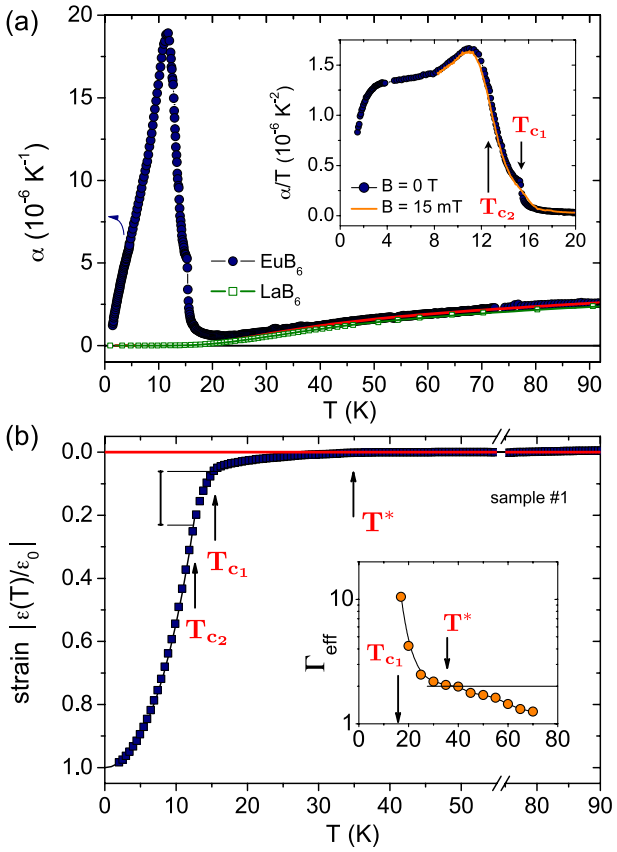

FIG. 1 (color online). (a) Coefficient of thermal expansion $\alpha(T)$ vs T of EuB_6 (blue circles) and LaB_6 (green squares). Red line represents the estimated phonon contribution for EuB_6 as described in the text. Inset shows the same data in a plot α/T vs T together with data at a field of $B = 15$ mT. (b) Modulus of the (negative) spontaneous strain $\epsilon = (\Delta l/l)_{EuB_6} - (\Delta l/l)_{\mathrm{ph}}$ vs T normalized to the value at zero temperature $\epsilon_0 \sim 300 \times 10^{-6}$. Arrows indicate the transition temperatures T_{c_1} and T_{c_2} (scale bar indicates the strain in this temperature interval) as well as the characteristic temperature for magnetic polaron formation T^*. Inset shows Γ_{eff} (see text) for $T > T_{c_1}$.

corresponding to a spontaneous strain, normalized to the extrapolated value at zero temperature ϵ_0, which amounts to $\epsilon_0 \sim 300 \times 10^{-6}$. Our data uncover the onset of the negative strain at a temperature around $T^* \sim 35$ K. Remarkably, this is the same temperature below which indications for bound MPs have been observed [16,18–20], suggesting that their formation is accompanied by a lattice distortion. Upon further cooling, the lattice contraction strongly increases at the percolation transition temperature T_{c_1}, and then displays an order parameterlike behavior below T_{c_2} (solid line). Furthermore, we find that about 15%–20% of the spontaneous lattice contraction occurs between T_{c_1} and T_{c_2} [see the scale bar in Fig. 1(b)], which, remarkably, is also the amount of Eu moments that already order at T_{c_1} before bulk FM order sets in [16].

Indications for an anomalous contribution to the expansivity below T^* can be found also by looking at the effective

Grüneisen parameter $\Gamma_{\rm eff} = (V_{\rm mol}/\kappa_T)(3\alpha_{\rm EuB_6}/C_V) = (V_{\rm mol}/\kappa_T)[3(\alpha_{\rm ph} + \alpha_{\rm mag})/C_V]$ [27] shown in the inset of Fig. 1(b). Here $V_{\rm mol} = 43.9$ cm^3/mol is the molar volume, $\kappa_T = 0.6 \times 10^{-11}$ Pa^{-1} is the isothermal compressibility of EuB_6 [30], $\beta = 3\alpha$ is the volume expansion coefficient, and C_V is the specific heat [15,17,31]. The so-derived $\Gamma_{\rm eff} = \sum_i \Gamma_i C_{Vi}/\sum_i C_{Vi}$ is well defined in the PM region $T > T_{c_1}$ and consists of contributions from each subsystem Γ_i, such as i denoting lattice, electronic, and magnetic, weighted by its specific heat C_{Vi}. $\Gamma_{\rm eff}$ is usually of order unity for simple metals or insulators [32]. As shown in the inset of Fig. 1(b), $\Gamma_{\rm eff}$ approaches 1 for $T > 70$ K and gradually increases upon cooling, reaching an enhanced value of $\Gamma_{\rm eff} \sim 2$ around 40 K (close to T^*). Hence, far above T^*, in the PM regime, $\Gamma_{\rm eff}$ is consistent with a phonon-dominated anharmonicity. In the regime of isolated MPs, $T_{c_1} \leq T \leq T^*$, we observe an increase from 2 at 40 K to $\Gamma_{\rm eff} \sim 5$ at around $T = 20$ K. Finally, the drastic enhancement of $\Gamma_{\rm eff}$ on approaching the FM regime for $T < 20$ K is strongly influenced by percolating MPs and charge delocalization, as we will argue below.

Further evidence for an anomalous contribution to the lattice strain can be found by studying the effect of a magnetic field on $\alpha(T)$ at low temperatures, shown in Fig. 2 for a selection of magnetic fields. Whereas the transition at T_{c_1} is strongly influenced by the magnetic field [33] the pronounced peak associated with T_{c_2} is much less field dependent. With increasing field, the peak becomes suppressed in magnitude and develops into a rounded maximum with a progressively broadened high-temperature tail, whereas its position slightly shifts to higher temperatures. In order to separate from $\alpha_{\rm mag}$ the ordinary exchange striction-type contribution of local-moment magnetic ordering, we compare the data with model calculations for a local-moment ferromagnet with nearest neighbor exchange J. Within mean-field (MF) theory, a magnetic contribution $(\Delta l/l)^{\rm MF}_{\rm loc} \propto M^2_{\rm loc}$ is expected, with $M_{\rm loc}$ the magnetization, see Refs. [34,35] and references cited therein. This results in

$$\alpha^{\rm MF}_{\rm loc}(T,B) = cM_{\rm loc}(T,B)\frac{\partial M_{\rm loc}(T,B)}{\partial T}. \qquad (1)$$

Here $M_{\rm loc}(T,B)$ is obtained from solving the Brillouin function for $S = 7/2$ at various magnetic fields B and c is a constant proportional to the local-moment magnetic Grüneisen parameter. As shown by the solid lines in Fig. 2, this model, with c as the only adjustable parameter, provides an excellent description of the data at 5 T for $T \lesssim 30$ K. At this magnetic field level, MPs are widely suppressed as deduced, e.g., from magnetoresistance measurements [15], and a homogeneous magnetic state develops. By using the same constant c [35], parameter-free model curves can then be calculated for all other fields depicted in Fig. 2. The figure shows that these curves for fields $B < 5$ T provide a reasonably good description of $\alpha_{\rm mag}$ only at its low-temperature end, i.e., sufficiently deep in the FM state, but deviate considerably at intermediate temperatures and for the high-temperature tail. For small fields $B \lesssim 500$ mT, these deviations are particularly strong around 15 K, corresponding to $T_{c_1}(B = 0)$, below which MPs percolate, i.e., where also the CMR effect is largest [16,17].

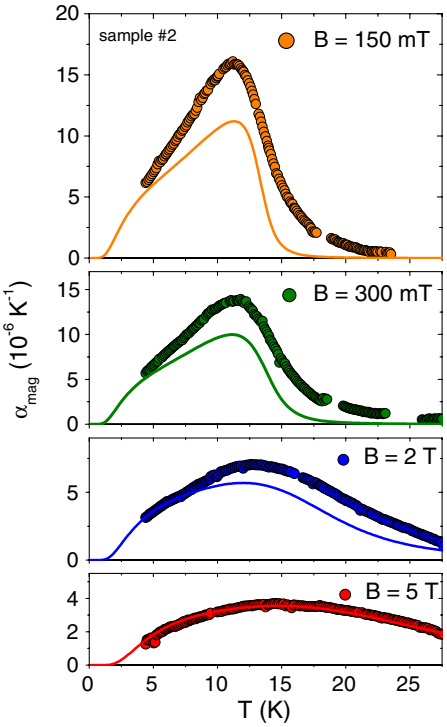

FIG. 2 (color online). Magnetic field dependence of the magnetic contribution to the thermal expansion coefficient $\alpha_{\rm mag}(T) = \alpha_{\rm EuB_6}(T) - \alpha_{\rm ph}(T)$, where a small phonon part is subtracted. Solid lines are mean-field calculations for a local-moment ferromagnet with $S = 7/2$ and $T_C = 12.6$ K.

Such an interrelation of an anomalous lattice strain and the CMR effect for $T_{c_2} < T \lesssim T_{c_1}$ is corroborated by magnetostriction measurements. In Fig. 3(a) we show the B-induced relative length change at various constant temperatures in the FM and PM regimes. The data in the FM regime, e.g., at $T = 11$ K, reveal a considerable B-induced contraction, well accounted for by local-moment FM ordering in the mean-field model. However, a distinctly stronger effect is observed by slightly increasing the temperature to 13.5 K, i.e., between T_{c_1} and T_{c_2}, the polaronic percolation regime. Remarkably, $\Delta l/l$ vs B is largest at $T \sim 15$ K, i.e., close to $T_{c_1}(B = 0)$, where also the CMR effect is largest. These observations, together with the strikingly similar shapes of the magnetostriction λ and differential magnetoresistance dR/dB curves in Figs. 3(b) and 3(c), respectively, suggest a close interrelation between lattice strain and field-induced charge carrier delocalization. Figure 3(d) compiles in a B-T diagram the positions of

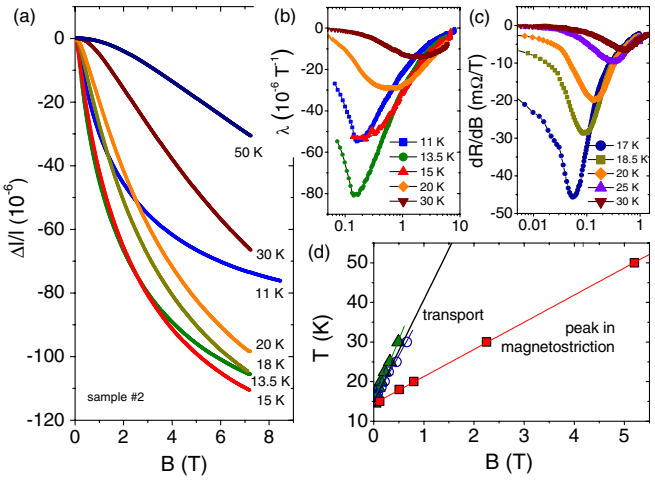

FIG. 3 (color online). (a) Relative length change as a function of applied magnetic field, $\Delta l/l$ vs B, at different constant temperatures and (b) the corresponding magnetostriction coefficient $\lambda = \partial \ln l/\partial B$. (c) Magnetic field derivative of the magnetoresistance at various temperatures. (d) B-T diagram showing the peaks in the magnetostriction coefficient λ (red squares) with a linear fit (red line) to the data. Also shown is the carrier delocalization transition as determined from the switching field of the Hall resistivity (black line) [14], which nearly coincides with the peak in the temperature derivative of the magnetoresistance (green triangles) [see (c)] and a peak in nonlinear transport (open circles) [36].

the minima in $\lambda(B)$ (this work) and $dR(B)/dB$ [36] for different temperatures, together with anomalies in nonlinear magnetotransport [18,36] and the signatures of charge delocalization in the PM regime as deduced from the Hall effect [14]. Strikingly, they all exhibit an in-B-linear behavior, which for $B \to 0$ extrapolates to the upper transition T_{c_1}, related to the charge delocalization. Since this temperature also coincides with the PM Curie temperature Θ_p, the anomalies in the various quantities occur at a constant value of $B_c/(T - \Theta_p)$, which in turn is proportional to the magnetization in the PM phase (Curie-Weiss law). We find that the crossover field B_c, and thus the critical magnetization, is different for thermodynamic and transport quantities.

The above measurements on EuB_6 reveal anomalous contributions to the lattice strain both as a function of T and B, which can be assigned to the stabilization and subsequent percolation of MPs. Upon cooling in zero field, this anomalous lattice strain sets in at T^*, where bound MPs become stabilized. This may be explained by local lattice distortions surrounding these isolated objects caused by the Coulomb effects from the surrounding point charges of the lattice acting on them. This effect, which describes the influence of fourth-order CEF splitting on the variation of the exchange constant between neighboring Eu^{2+} ions with the lattice parameters, has been estimated in Ref. [37]. It is found that this effect alone cannot explain the large lattice contraction at the low-temperature transitions T_{c_1} and T_{c_2} [38], in agreement with a substantial contribution from charge delocalization: upon cooling, the MPs grow in size (and possibly number) until at T_{c_1} the percolation threshold is reached and the holes become delocalized. This sudden increase of "metallicity" goes along with the formation of an infinite magnetic cluster, involving the ordering of 15%–20% of the magnetic moments as the percolation progresses until T_{c_2} is reached, where the magnetic clusters merge. Below T_{c_2}, the process of charge delocalization levels off and spontaneous magnetization due to local moment FM exchange prevails. This substantial lattice strain accompanying the magnetically driven delocalization of charges is similar to what is observed across the Mott metal-insulator transition in molecular conductors [40]. In both cases, the charge delocalization, which strengthens the chemical binding, may account for the pronounced lattice contraction.

For finite magnetic fields, an additional contribution to the expansivity is observed in the PM temperature region, see Fig. 2. The coincidence of the temperatures, where both the magnetostriction and the CMR effect are largest (see Fig. 3), suggests a common origin, namely magnetically driven charge delocalization. The fact that in the PM regime this effect is a crossover rather than a phase transition may explain why the anomalies in transport and thermodynamic properties occur at different values of a critical magnetization [different slopes in Fig. 3(d)], a behavior that is observed also in other materials with large negative magnetoresistance [41].

So far, in Eu-chalcogenide alloys and magnetic semiconductors, and also for the present EuB_6, MPs have been assumed to be unaccompanied by lattice distortions [1,6,42]. However, our results highlight a close interrelation of transport, magnetic, and elastic properties. Comparing these findings for a simple material like EuB_6, which is devoid of additional JT lattice distortion or strong CEF effects, with the observations for the manganites and other CMR systems suggests that a strong effect of the formation and dynamics of magnetic clusters on the lattice parameters is a general feature of CMR materials.

*Present address: Experimentalphysik VI, Center for Electronic Correlations and Magnetism, Augsburg University, 86159 Augsburg, Germany.
†Present address: Department of Physics, Indian Institute of Technology, New Dehli, India.
‡Present address: IGCE, Universidade Estadual Paulista, Departamento de Física, Rio Claro, Brazil.
§j.mueller@physik.uni-frankfurt.de

[1] S. von Molnár and S. Methfessel, J. Appl. Phys. **38**, 959 (1967).
[2] A. P. Ramirez and M. A. Subramanian, Science **277**, 546 (1997).

[3] *Colossal Magnetoresistance, Charge Ordering and Related Properties of Manganites*, edited by C. N. R. Rao and B. Raveau (World Scientific, Singapore, 1998).
[4] A. Kaminski and S. Das Sarma, Phys. Rev. Lett. **88**, 247202 (2002).
[5] H. Li, Y. Xiao, B. Schmitz, J. Persson, W. Schmidt, P. Meuffels, G. Roth, and T. Brückel, Sci. Rep. **2**, 750 (2012).
[6] T. Kasuya and A. Yanase, Rev. Mod. Phys. **40**, 684 (1968).
[7] J. M. De Teresa, M. R. Ibarra, P. A. Igarabel, C. Ritter, C. Marquina, J. Blasco, J. Garcia, A. del Moral, and Z. Arnold, Nature (London) **386**, 256 (1997).
[8] M. R. Ibarra, P. A. Algarabel, C. Marquina, J. Blasco, and J. Garcia, Phys. Rev. Lett. **75**, 3541 (1995).
[9] B. García-Landa, C. Marquina, M. R. Ibarra, G. Balakrishnan, M. R. Lees, and D. McK. Paul, Phys. Rev. Lett. **84**, 995 (2000).
[10] J. A. Souza, Yi-Kuo Yu, J. J. Neumeier, H. Terashita, and R. F. Jardim, Phys. Rev. Lett. **94**, 207209 (2005).
[11] L. Downward, F. Bridges, S. Bushart, J. Neumeier, N. Dilley, and L. Zhou, Phys. Rev. Lett. **95**, 106401 (2005).
[12] H. D. Zhou, E. S. Choi, J. A. Souza, J. Lu, Y. Xin, L. L. Lumata, B. S. Conner, L. Balicas, J. S. Brooks, J. J. Neumeier, and C. R. Wiebe, Phys. Rev. B **77**, 020411(R) (2008).
[13] Z. Fisk, D. C. Johnston, B. Cornut, S. von Molnár, S. Oseroff, and R. Calvo, J. Appl. Phys. **50**, 1911 (1979).
[14] X. Zhang, L. Yu, S. von Molnár, Z. Fisk, and P. Xiong, Phys. Rev. Lett. **103**, 106602 (2009).
[15] S. Süllow, I. Prasad, M. C. Aronson, J. L. Sarrao, Z. Fisk, D. Hristova, A. H. Lacerda, M. F. Hundley, A. Vigliante, and D. Gibbs, Phys. Rev. B **57**, 5860 (1998).
[16] S. Süllow, I. Prasad, M. C. Aronson, S. Bogdanovich, J. L. Sarrao, and Z. Fisk, Phys. Rev. B **62**, 11626 (2000).
[17] R. R. Urbano, P. G. Pagliuso, C. Rettori, S. B. Oseroff, J. L. Sarrao, P. Schlottmann, and Z. Fisk, Phys. Rev. B **70**, 140401(R) (2004).
[18] P. Das, A. Amyan, J. Brandenburg, J. Müller, P. Xiong, S. von Molnár, and Z. Fisk, Phys. Rev. B **86**, 184425 (2012).
[19] P. Nyhus, S. Yoon, M. Kauffman, S. L. Cooper, Z. Fisk, and J. Sarrao, Phys. Rev. B **56**, 2717 (1997).
[20] M. L. Brooks, T. Lancaster, S. J. Blundell, W. Hayes, F. L. Pratt, and Z. Fisk, Phys. Rev. B **70**, 020401(R) (2004).
[21] N. N. Sirota, V. V. Novikov, and A. A. Sidorov, Phys. Solid State **42**, 199 (2000).
[22] S. Zherlitsyn, B. Wolf, B. Lüthi, M. Lang, P. Hinze, E. Uhrig, W. Assmus, H. R. Ott, D. P. Young, and Z. Fisk, Eur. Phys. J. C **22**, 327 (2001).
[23] H. Martinho, C. Rettori, G. M. Dalpian, J. L. F. da Silva, Z. Fisk, and S. B. Oseroff, J. Phys. Condens. Matter **21**, 456007 (2009).
[24] C. H. Booth, J. L. Sarrao, M. F. Hundley, A. L. Cornelius, G. H. Kwei, A. Bianchi, Z. Fisk, and J. M. Lawrence, Phys. Rev. B **63**, 224302 (2001).
[25] R. Pott and R. Schefzyk, J. Phys. E **16**, 444 (1983).
[26] M. Peschke, Diploma Thesis, Technical University Darmstadt, 1985 (unpublished).
[27] We neglect the very small linear contribution of free charge carriers.
[28] D. Mandrus, B. C. Sales, and R. Jin, Phys. Rev. B **64**, 012302 (2001).
[29] See Supplemental Material at http://link.aps.org/supplemental/10.1103/PhysRevLett.113.067202 for a detailed description of how the phonon background is determined.
[30] T. Lundström, B. Lönnberg, and B. Törmä, Phys. Scr. **26**, 414 (1982).
[31] T. Fujita, M. Suzuki, and Y. Isikawa, Solid State Commun. **33**, 947 (1980).
[32] T. H. Barron, J. G. Collins, and G. K. White, Adv. Phys. **29**, 609 (1980).
[33] Already for $B \geq 15$ mT, the anomaly becomes very broad and slightly shifts to higher temperatures [see Fig. 1(a)] consistent with specific heat and electronic transport results [17].
[34] J. Fernández Rodríguez and J. A. Blanco, Phys. Scr. **71**, CC19 (2005).
[35] O. Heyer, P. Link, D. Wandner, U. Ruschewitz, and T. Lorenz, New J. Phys. **13**, 113041 (2011).
[36] A. Amyan, P. Das, J. Müller, and Z. Fisk, J. Korean Phys. Soc. **62**, 1489 (2013).
[37] C. N. Guy, S. von Molnár, J. Etourneau, and Z. Fisk, Solid State Commun. **33**, 1055 (1980).
[38] Assuming a nearest-neighbor point-charge model with a charge of -2 at the ligand site [39], however, a rough estimate using the parameters given in Ref. [37] yields $\Gamma_{\mathrm{eff}} \sim 4$–$6$, which indeed is observed at around $T = 20$ K.
[39] K. C. Turberfield, L. Passell, R. J. Birgeneau, and E. Bucher, Phys. Rev. Lett. **25**, 752 (1970).
[40] M. de Souza, A. Brühl, Ch. Strack, B. Wolf, D. Schweitzer, and M. Lang, Phys. Rev. Lett. **99**, 037003 (2007).
[41] S. V. Demishev, V. V. Glushkov, I. I. Lobanova, M. A. Anisimov, V. Yu. Ivanov, T. V. Ishchenko, M. S. Karasev, N. A. Samarin, N. E. Sluchanko, V. M. Zimin, and A. V. Semeno, Phys. Rev. B **85**, 045131 (2012).
[42] S. von Molnár, A. Briggs, J. Flouquet, and G. Remenyi, Phys. Rev. Lett. **51**, 706 (1983).